中国激光

集成DBR反馈区的1.3 μm高速直接调制InGaAlAs/InP DFB激光器

朱旭愿[1,2,3]，刺晓波[1,2,3]，郭竟[1,2,3]，李振宇[1,2,3]，赵玲娟[1,2,3]，王圩[1,2,3]，梁松[1,2,3*]

[1]中国科学院半导体研究所半导体材料科学重点实验室，北京 100083；

[2]中国科学院大学材料与光电研究中心，北京 100049；

[3]低维半导体材料与器件北京市重点实验室，北京 100083

摘要 研制了以InGaAlAs多量子阱为有源材料的InP基1.3 μm波段高速直接调制分布反馈(DFB)激光器，单片集成了与DFB激光器区具有相同量子阱材料的分布式布拉格反射器(DBR)反馈区。室温下DFB有源区长度为200 μm时器件的3 dB小信号直接调制带宽大于29 GHz。在速率为25 Gbit/s的非归零(NRZ)码数据调制下，光信号经10 km长的单模光纤传输后获得10^{-10}误码率的功率代价在室温及80 ℃下均小于1 dB。激光器的有源区长度较大，有利于提高发光效率并且有助于减小电流热效应的不利影响。所研制的高速直接调制激光器是大容量短距光纤通信系统的理想光源，具有广阔的应用前景。

关键词 激光器；半导体激光器；高速直接调制；InGaAlAs/InP量子阱；1.3 μm波段

中图分类号 TN248.4 **文献标志码** A **DOI**: 10.3788/CJL220827

1 引 言

近年来，云计算及高清视频等业务的迅速发展推动光纤通信网络数据传输容量的爆炸性增加[1]。高速半导体激光器是大容量短距光纤通信系统的理想光源，具有体积小、功耗低、成本低等优点[2-5]。半导体激光器加载调制信号的方法主要有外调制和直接调制两种方式。其中，外调制方式是将调制信号加载至分立的调制器上，例如，$LiNbO_3$电光调制器[6-7]及半导体电吸收调制器[8-10]，而直接调制方式是将调制信号直接加载至激光器的驱动电流上[11-13]。相较于外调制方式，直接调制激光器具有更低成本和更高功率，同时系统的复杂度也较低[14]。

提高光纤通信系统容量的一个方法是提高半导体激光器的调制带宽。一般来说，半导体激光器的3 dB直接调制带宽(f_{3dB})与弛豫振荡频率(f_r)的关系可表示为$f_{3dB}=1.55f_r$[15]。为了提高直接调制带宽，首先需要采用高增益有源区材料来制作半导体激光器[13]。在这方面，InGaAlAs多量子阱(MQWs)材料是一个理想的选择，其高微分增益及较大的阱垒导带带隙差均有利于提高激光器性能。另一方面，减小器件的腔长可以减小激光器反馈腔内的光子寿命，从而也可以提高激光器的调制带宽[13]。

鉴于其重要应用价值，高速直接调制分布反馈(DFB)半导体激光器是国内外高速光电子器件领域的研究热点之一。日本NTT公司研制了集成无源波导的1.3 μm波段InP基InGaAlAs量子阱脊型波导DFB激光器，直接调制带宽达34 GHz[16]。美国Lumentum公司2021年报道了应用于粗波分复用(CWDM)光通信的1.3 μm波段高速直接调制激光器，该激光器采用高限制因子InGaAlAs量子阱材料及非均匀周期光栅结构，在2 km单模光纤中实现了106 Gbit/s的数据传输[17]。国内相关机构也开展了相关研究，其中华中科技大学报道了采用有源反馈结构的1.3 μm波段InGaAlAs量子阱激光器，实现了宽温度范围内的25 Gbit/s数据加载[18]。为了获得高直接调制带宽，已报道的多数激光器的有源区长度为150 μm，甚至100 μm[16-18]。较小的有源区长度给激光器的制作及使用都带来了一些潜在问题。一方面，腔长的缩短相当于增加了激光器的腔面损耗，不利于提高激光器的发光效率。另一方面，腔长越短，激光器的串联电阻越大，工作时电流产生的热越多，不利于器件在高温时的正常工作，对器件的可靠性也可能产生不利影响。

集成分布式布拉格反射器(DBR)反馈区是高速直调激光器常用的方案[19]，DBR反馈区给DFB激光

收稿日期：2022-05-07；**修回日期**：2022-06-06；**录用日期**：2022-06-27；**网络首发日期**：2022-07-07

基金项目：国家重点研发计划(2018YFB2200801)

通信作者：*liangsong@semi.ac.cn

器区提供了光反馈：一方面起到高反镀膜的作用，有利于减小阈值电流并提高光输出功率；另一方面减小了解理端面相位不确定性的影响，可以显著提升激光器的单模成品率。本文报道了单片集成DBR反馈区的高速直调InP基1.3 μm波段InGaAlAs量子阱DFB激光器，其DFB区及DBR反馈区具有相同的量子阱材料，无须使用对接生长等单片集成技术，因此器件制作工艺得到了有效的简化。室温条件下所研制的激光器在DFB有源区长度为200 μm时即可获得大于29 GHz的直接调制带宽，在速率为25 Gbit/s的非归零（NRZ）码数据调制下，光信号经10 km长的单模光纤传输后获得10^{-10}误码率的功率代价在室温及80 ℃下均小于1 dB。

2 器件结构与制备

利用金属有机化学气相沉积（MOCVD）法在n-InP衬底上生长激光器材料。在第一次MOCVD过程中，生长多量子阱有源材料，包含9个4 nm厚的压应变（$+1.2\times10^{-2}$）InGaAlAs阱和10个10 nm厚的张应变（-2×10^{-3}）InGaAlAs垒层。多量子阱结构上下均为总厚度为100 nm的InGaAlAs材料层，都包括一个50 nm厚的InGaAlAs折射率渐变（GRIN-InGaAlAs）层及一个50 nm厚的InAlAs材料层。在InAlAs材料上生长了厚度为60 nm的InGaAsP材料以制作DFB光栅结构。图1(a)为量子阱有源材料的X射线衍射（XRD）曲线，清晰的高阶衍射峰说明量子阱具有较高的晶体质量。图1(b)为材料室温下的光致发光光谱，其峰值波长为1300 nm，光谱的半峰全宽为40 nm。在光栅层材料内采用电子束曝光（EBL）和干法刻蚀技术制作了光栅结构，光栅刻蚀深度为50 nm，周期为204 nm。在第二次MOCVD过程中，依次沉积p型InP盖层和p型InGaAs接触层，完成了器件制作所需的完整材料结构，其折射率分布如图1(c)所示，其中x表示从衬底开始的外延材料的厚度。

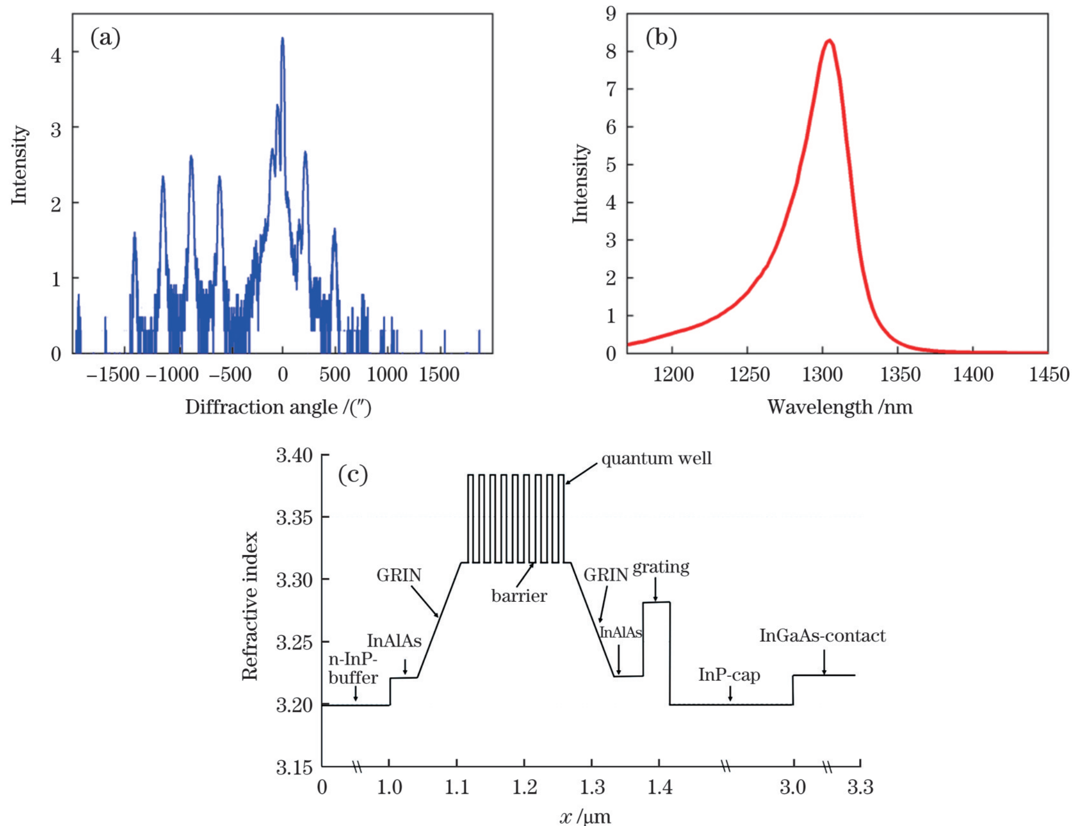

图1 InGaAlAs/InP多量子阱。(a)XRD曲线；(b)光致发光光谱；(c)器件的折射率分布

Fig.1 InGaAlAs/InP multi-quantum wells. (a) XRD curve ; (b) photoluminescence spectrum; (c) refractive index distribution of device

图2为制作的直接调制DFB激光器截面结构示意图及其光学显微镜（OM）照片，其中λ为布拉格波长，I_{DFB}表示DFB区的偏置电流，AR表示抗反射。器件采用脊型波导结构，包括一段长度为200 μm或150 μm的DFB激光器区及一段长度为130 μm的DBR反馈区，脊波导宽度均为1.7 μm。如图2(a)所示，第一次MOCVD过程中生长的InGaAlAs量子阱材料同时作为DFB区的增益材料及DBR反馈区的波导材料。器件的两个区域内的光栅具有相同的周期和刻蚀深度，为了提高器件的单模成品率，在DFB区的中间位置制作了1/4波长相移结构。DFB区的注入电流超过阈值电流时该区产生激光发射，DBR反馈区的光栅将光入射到反馈区内的光反射回DFB区，起到了提高光输出功率的作用。此外，DBR反馈区减小了解理端面相位

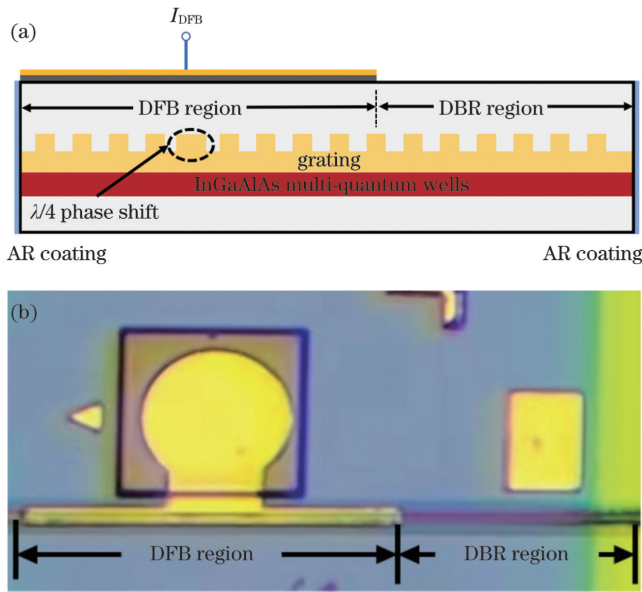

图 2　器件结构。(a)截面结构示意图;(b)光学显微镜照片

Fig.2　Device structure. (a) Structural diagram of section; (b) OM image

不确定性的影响,可以有效提升激光器的单模成品率[20]。与采用对接生长等技术制作的集成DBR反馈区的器件相比[21],本文设计的器件DFB区及DBR反馈区采用了相同的量子阱材料,器件制作的工艺得到有效简化。在芯片的反馈区没有制作电极,为了减小DFB区电流向反馈区的扩散,去除了反馈区波导上部的InGaAs接触层材料。激光器电极焊盘直径为80 μm,为了减小寄生电容对调制带宽的影响,在焊盘下制作了厚度为2.6 μm的聚酰亚胺材料层。在激光器两个端面镀制增透膜后,将芯片烧结于AlN热沉上进行测试。

3　器件性能

图3(a)为20 ℃下激光器发光功率(P)随注入电流(I)的变化曲线。可以看出,DFB区长度为200 μm时器件阈值电流为12 mA,100 mA电流下的发光功率可以达到18 mW。器件光反馈区也存在量子阱材料,在DFB区发光功率较低时,DBR反馈区提供光反馈,同时也对光产生一定的吸收,随着DFB区发光强度的增加,反馈区对光的吸收很快饱和,之后仅提供光反馈[18],这个过程导致了P-I曲线中20 mA电流附近斜率拐点的出现。在60 mA电流以上时,发光功率的饱和是由电流的热效应引起的。DFB区长度为150 μm时器件阈值电流增加至17 mA,100 mA电流下的发光功率与DFB区长度为200 μm的器件相比也有所下降,表明短有源区长度有不利影响。图3(b)为在不同电流下测得的DFB区长度为200 μm的器件的激射光谱。可见器件激射波长在1320 nm附近,所测试的电流范围内的边模抑制比均大于50 dB,显示了良好的单模特性。当电流由30 mA增加至90 mA时,激射波长由1317.82 nm增加至1319.91 nm,其随电流的变化速率为0.035 nm/mA。由图3(b)可知,光谱截止带宽度为3 nm,其与光栅耦合系数(κ)的关系为

$$\kappa = \pi \frac{n_{\mathrm{eff}} \lambda_{\mathrm{s}}}{\lambda_{\mathrm{B}}^{2}}, \tag{1}$$

式中:材料有效折射率n_{eff}为3.22;激射波长λ_{B}为1320 nm。可以得到激光器光栅耦合系数为175 cm^{-1}。

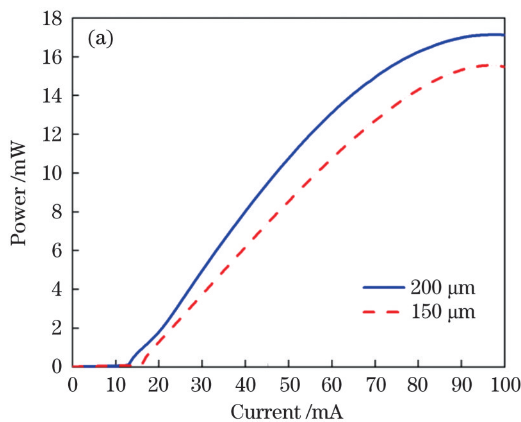

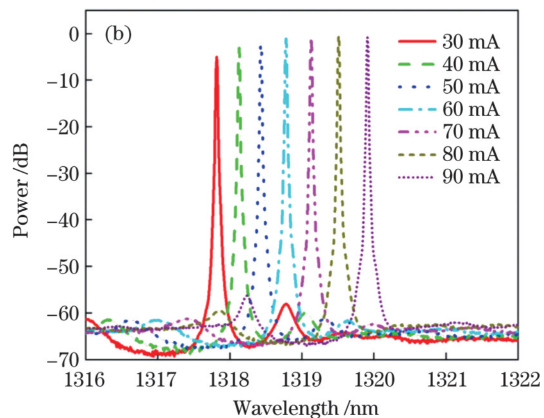

图 3　功率-电流曲线及测试光谱。(a)室温下不同DFB区长度下的功率-电流曲线;(b)不同电流下DFB区长度为200 μm的器件的激射光谱

Fig.3　Power-current curves and measured spectra. (a) Power-current curves of devices with different DFB region lengths at room temperature; (b) excitation spectra of device with DFB region length of 200 μm under different currents

利用带宽为50 GHz的矢量网络分析仪测试了器件的小信号直接调制响应特性。图4(a)为20 ℃时不同电流下测得的DFB区长度为200 μm时器件的小信号直接调制响应曲线。3 dB小信号调制带宽随注入电流的增加而增大,注入电流为60 mA时3 dB小信号调制带宽为20 GHz,注入电流为94 mA时3 dB小信号调制带宽增大至29 GHz以上。由图4(a)还可以看出,在所有测试电流下,直接调制响应曲线均较平坦,弛豫振荡频率附近的最高点均低于2.5 dB。图4(b)为DFB区长度为150 μm时器件的调制响应曲线。可见,

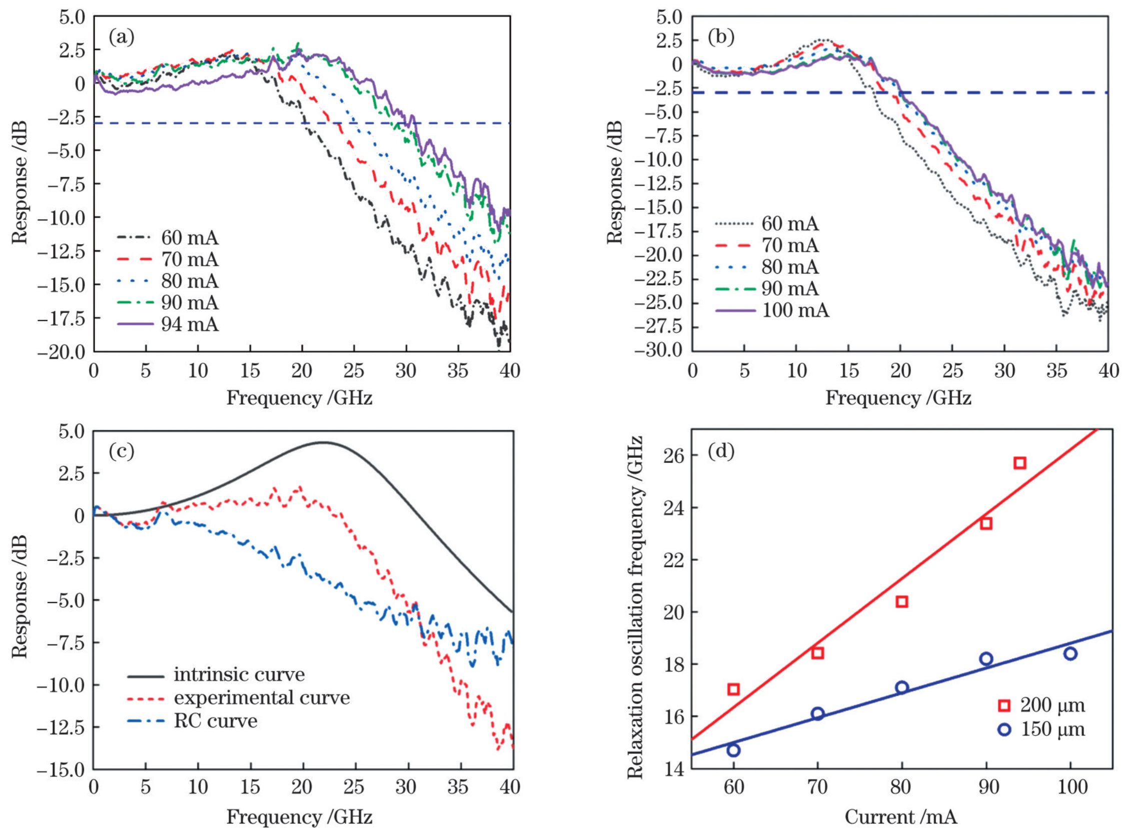

图 4　器件的小信号直接调制响应。(a)DFB 区长度 200 μm;(b)DFB 区长度 150 μm;(c)DFB 区长度为 200 μm 时 94 mA 电流下的拟合结果;(d)激光器的弛豫振荡频率随电流的变化

Fig.4　Small signal direct modulation response of device. (a) DFB region with 200 μm length; (b) DFB region with 150 μm length; (c) fitting results under 94 mA current when length of DFB region is 200 μm; (d) relaxation oscillation frequency versus current

电流为 60 mA 时调制带宽为 17 GHz,电流为 80 mA 时调制带宽增大至 19 GHz,继续增加驱动电流,带宽发生饱和。80 mA 注入电流下 DFB 区长度为 200 μm 及 150 μm 时器件的串联电阻分别为 8 Ω 及 13 Ω。尽管短腔长有利于提高器件的调制带宽,但短腔长带来的高电阻会产生更显著的热效应,恶化了器件的高频调制特性。

通过将不同偏置电流下测得的两条频率响应曲线相减,对实验获得的小信号响应曲线进行了拟合[22],DFB 区长度为 200 μm 时 94 mA 电流下的拟合结果如图 4(c)所示。拟合获得的扣除 RC 响应影响的器件本征小信号响应带宽为 35.4 GHz,显著高于实验测得的带宽。可见通过进一步优化寄生电容等参数,器件的直接调制带宽可以得到进一步的提高。通过拟合还可以获得器件的弛豫振荡频率,其随激光器电流的变化如图 4(d)所示,DFB 区长度为 200 μm 和 150 μm 时变化率分别为 0.25 GHz/mA 和 0.09 GHz/mA。为了获得 25 GHz 的带宽,国内外已报道的大多数直接调制激光器的有源区长度都小于 150 μm[13-15]。相比之下,本文报道的 DFB 区长度为 200 μm 时的带宽即可超过 29 GHz,长腔长有利于提高激光器的发光效率,并有助于减小电流热效应对器件的不利影响。

利用所研制的 DFB 区长度为 200 μm 的芯片进一步开展了数据传输实验,调制信号为速率为 25.78 Gbit/s 的非归零伪随机码,码长为 $2^{15}-1$,信号幅度为 ±40 mA。图 5 为 20 ℃和 80 ℃下背对背(BTB)传输及经过 10 km 长标准单模光纤(SMF)传输后的眼图。可见,在所有实验条件下眼图均清晰张开。20 ℃下 BTB 及 10 km 长光纤传输后的动态消光比分别为 7.16 dB 及 6.87 dB,80 ℃下 BTB 及 10 km 长光纤传输后的动态消光比分别为 8.1 dB 及 7.57 dB。在速率为 25.78 Gbit/s 的 NRZ 数据调制下的误码测(B_r)试结果如图 6 所示,在 20 ℃和 80 ℃下经 10 km 长单模光纤传输后获得 10^{-10} 误码率的功率代价均小于 1 dB。

4　结　　论

报道了集成 DBR 反馈区的高速直调 InP 基 1.3 μm 波段 InGaAlAs 量子阱 DFB 激光器。由于 DBR 反馈区采用与 DFB 区相同的量子阱材料,器件的制作工艺得到了有效的简化。当器件 DFB 区长度为 200 μm 时,在室温条件下获得了大于 29 GHz 的直接调制带宽。较大的有源区长度有利于提高激光器的发光效率并且有助于减小电流热效应对器件的不利影响。在速度为 25 Gbit/s 的 NRZ 数据调制下,在 20 ℃和

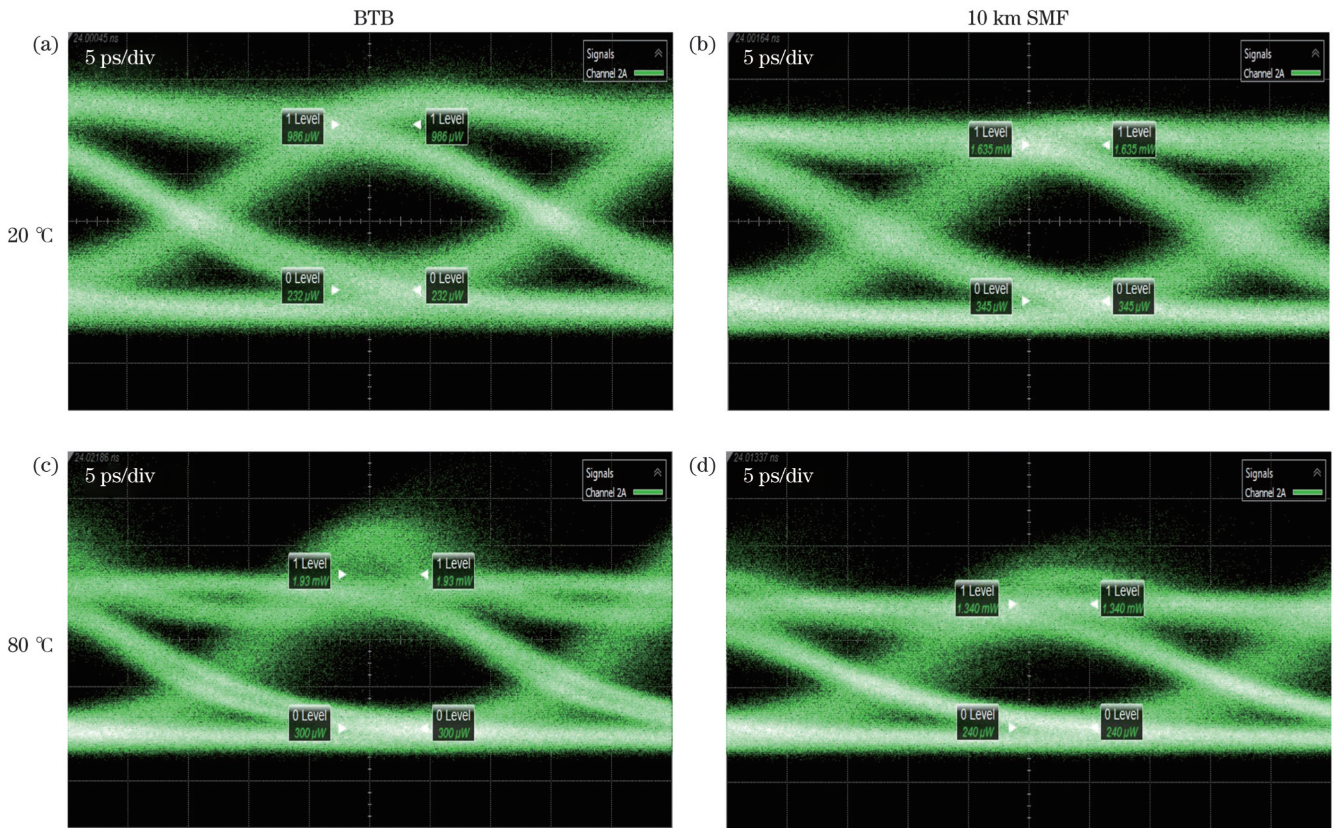

图 5　在速率为 25.78 Gbit/s 的 NRZ 数据调制下的眼图

Fig. 5　Eye views under NRZ data modulation at rate of 25.78 Gbit/s

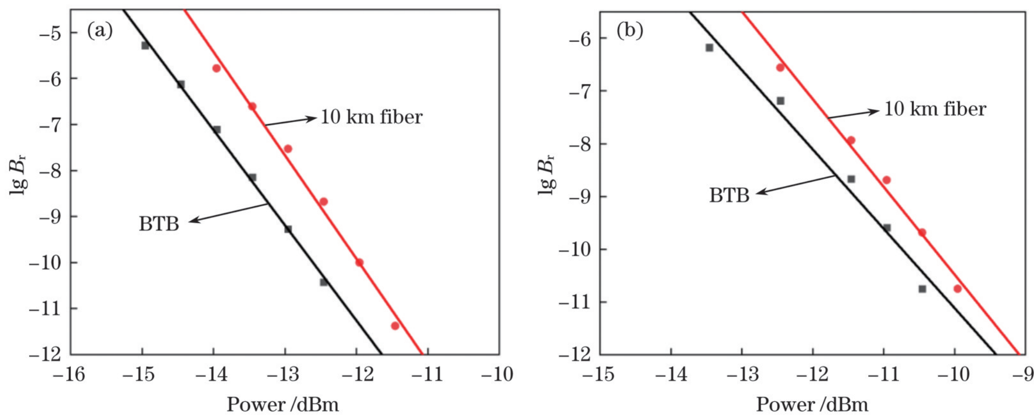

图 6　不同温度下的误码率测试结果。(a) 20 ℃；(b) 80 ℃

Fig.6　Measured bit-error-rate results under different temperatures. (a) 20 ℃; (b) 80 ℃

80 ℃下经 10 km 长单模光纤传输后获得 10^{-10} 误码率的功率代价均小于 1 dB。所研制的高速直调激光器是大容量短距光纤通信系统的理想光源，具有广阔的应用前景。

参　考　文　献

[1] Cisco U. Cisco annual Internet report (2018-2023) white paper[EB/OL]. (2020-03-09)[2022-02-04]. https://www.cisco.com/c/en/us/solutions/collateral/executive-perspectives/annual-internet-report/white-paper-c11-741490.html.

[2] Tucker R. High-speed modulation of semiconductor lasers[J]. Journal of Lightwave Technology, 1985, 3(6): 1180-1192.

[3] 陈良惠，杨国文，刘育衔. 半导体激光器研究进展[J]. 中国激光，2020, 47(5): 0500001.
Chen L H, Yang G W, Liu Y X. Development of semiconductor lasers[J]. Chinese Journal of Lasers, 2020, 47(5): 0500001.

[4] 袁庆贺，井红旗，刘素平，等. 导波模式对锥形半导体激光器输出特性的影响[J]. 中国激光，2021, 48(9): 0901001.
Yuan Q H, Jing H Q, Liu S P, et al. Influence of guided wave mode on output characteristics of tapered diode laser[J]. Chinese Journal of Lasers, 2021, 48(9): 0901001.

[5] 柯旭，邓乐武. 弱耦合互注入锁定半导体激光器的线宽研究[J]. 中国激光，2022, 49(3): 0301001.
Ke X, Deng L W. Linewidth of mutually injection-locked semiconductor lasers in weak coupling regime[J]. Chinese Journal of Lasers, 2022, 49(3): 0301001.

[6] Yamazaki H, Yamada T, Sakamaki Y, et al. Advanced optical modulators with hybrid configuration of silica-based PLC and $LiNbO_3$ phase-shifter array for ultra-high-speed transport networks

[C] // 2008 First ITU-T Kaleidoscope Academic Conference-Innovations in NGN: Future Network and Services, May 12-13, 2008, Geneva. New York: IEEE Press, 2008: 237-244.
[7] Doi Y, Yamada T. Recent progress on hybrid silica-PLCs/$LiNbO_3$ modulator for advanced transmission formats[C]//OECC 2010 Technical Digest, July 9-10, 2010, Sapporo, Japan. New York: IEEE Press, 2010: 564-565.
[8] Liu Y L, Zhang L C, La X B, et al. Up to 50 Gb/s modulation of an EAM integrated widely tunable DBR laser[J]. Optics Express, 2021, 29(3): 4523-4529.
[9] Liu Y L, Tang Q, Zhang L C, et al. Dual-wavelength DBR laser integrated with high-speed EAM for THz communications[J]. Optics Express, 2020, 28(7): 10542-10551.
[10] Deng Q F, Zhu H L, Xie X, et al. Low chirp EMLs fabricated by combining SAG and double stack active layer techniques[J]. IEEE Photonics Journal, 2018, 10(2): 7902007.
[11] Zhou D B, Liang S, Zhao L J, et al. High-speed directly modulated widely tunable two-section InGaAlAs DBR lasers[J]. Optics Express, 2017, 25(3): 2341-2346.
[12] Zhou D B, Liang S, He Y M, et al. Two 10 Gb/s directly modulated DBR lasers covering 20 nm wavelength range[J]. Optics Communications, 2020, 475: 126236.
[13] Tang Q, Liu Y L, Zhang L C, et al. 25 Gb/s directly modulated widely tunable 1.3 μm dual wavelength DFB laser for THz communication [J]. IEEE Photonics Technology Letters, 2020, 32(7): 410-413.
[14] Kobayashi W, Tadokoro T, Ito T, et al. High-speed operation at 50 Gb/s and 60-km SMF transmission with 1.3-μm InGaAlAs-based DML[C]//ISLC 2012 International Semiconductor Laser Conference, October 7-10, 2012, San Diego, CA, USA. New York: IEEE Press, 2012: 50-51.
[15] Bowers J, Hemenway B, Gnauck A, et al. High-speed InGaAsP constricted-mesa lasers[J]. IEEE Journal of Quantum Electronics, 1986, 22(6): 833-844.
[16] Kobayashi W, Ito T, Yamanaka T, et al. 50-Gb/s direct modulation of a 1.3-μm InGaAlAs-based DFB laser with a ridge waveguide structure[J]. IEEE Journal of Selected Topics in Quantum Electronics, 2013, 19(4): 1500908.
[17] Nakajima T, Onga M, Sekino Y, et al. 106-Gb/s PAM4 operation of directly modulated DFB lasers from 25 ℃ to 70 ℃ for transmission over 2-km SMF in the CWDM range[J]. Journal of Lightwave Technology, 2022, 40(6): 1815-1820.
[18] Liu G H, Zhao G Y, Zhang G, et al. Directly modulated active distributed reflector distributed feedback lasers over wide temperature range operation (−40 ℃ to 85 ℃)[J]. Chinese Optics Letters, 2020, 18(6): 061401.
[19] Zhao G Y, Sun J Q, Xi Y P, et al. Design and simulation of two-section DFB lasers with short active-section lengths[J]. Optics Express, 2016, 24(10): 10590-10598.
[20] Matsuda M, Uetake A, Simoyama T, et al. 1.3-μm-wavelength AlGaInAs multiple-quantum-well semi-insulating buried-heterostructure distributed-reflector laser arrays on semi-insulating InP substrate[J]. IEEE Journal of Selected Topics in Quantum Electronics, 2015, 21(6): 241-247.
[21] Matsui Y, Pham T, Ling W A, et al. 55-GHz bandwidth short-cavity distributed reflector laser and its application to 112-Gb/s PAM-4[C]//2016 Optical Fiber Communications Conference and Exhibition (OFC), March 20-24, 2016, Anaheim, CA, USA. New York: IEEE Press, 2016.
[22] Morton P A, Tanbun-Ek T, Logan R A, et al. Frequency response subtraction for simple measurement of intrinsic laser dynamic properties[J]. IEEE Photonics Technology Letters, 1992, 4(2): 133-136.

1.3-μm High-Speed Directly-Modulated InGaAlAs/InP DFB Laser with Integrated DBR Feedback Region

Zhu Xuyuan[1,2,3], La Xiaobo[1,2,3], Guo Jing[1,2,3], Li Zhenyu[1,2,3], Zhao Lingjuan[1,2,3], Wang Wei[1,2,3], Liang Song[1,2,3*]

[1] *Key Laboratory of Semiconductor Material Science, Institute of Semiconductors, Chinese Academy of Sciences, Beijing* 100083, *China*;
[2] *Center of Materials Science and Optoelectronics Engineering, University of Chinese Academy of Sciences, Beijing* 100049, *China*;
[3] *Beijing Key Laboratory of Low Dimensional Semiconductor Materials and Devices, Beijing* 100083, *China*

Abstract

Objective High-speed modulated semiconductor lasers are important light sources for high-capacity optical communication systems. Compared with externally modulated lasers, such as electro-absorption modulated distributed feedback (DFB) lasers, directly modulated DFB lasers have several advantages, including a simple structure, low cost, and low power consumption. A higher speed of data transmission of an optical communication system can be obtained using DFB lasers with a higher direct modulation bandwidth in the following ways. First, high-gain active materials such as InGaAlAs/InP multi-quantum wells (MQWs) can be used for the fabrication of lasers. Subsequently, a short laser cavity length can be used to realize a short photon lifetime in the cavity. Because of their important applications, high-speed directly-modulated InGaAlAs/InP MQW DFB lasers have been widely studied. However, to obtain a high modulation bandwidth, the length of the active region for most reported lasers must be less than 150 μm. A small active length leads to a high facet loss, and thus, a low optical power output. In addition, a small length results in high resistance, which leads to a strong self-heating effect. In this paper, we report high-speed directly-modulated DFB lasers integrated with a distributed Bragg reflector (DBR) section working at 1.3-μm wavelength. For the cavity length of 200 μm, the 3-dB small signal direct modulation bandwidth of the laser is larger than 29 GHz.

Methods This device is fabricated via two-step lower pressure metal organic chemical vapor deposition (MOCVD) growth. In the

first step, the active layer, a multi-quantum well structure comprising nine 1.2% compressively strained InGaAlAs wells and ten 0.2% tensile-strained InGaAlAs barriers, is grown. The thicknesses of each well and barrier are 4 nm and 10 nm, respectively. A 50-nm-thick InGaAlAs graded index layer and a 50-nm-thick InAlAs laser are grown on both sides of the MQW layer. A 60-nm-thick InGaAsP layer is grown on the upper InAlAs layer for grating fabrication. After a uniform grating is fabricated using electron beam lithography and dry etching, an InP cladding layer and an InGaAs contact layer are grown in the second growth step. Figure 2 shows a schematic of the cross-section structure and an optical graph of the fabricated laser. The laser has a 1.7-μm-wide ridge waveguide structure and consists of a 200-μm-long DFB section and 130-μm-long DBR section. The gratings of the two sections have the same period and etching depth. To obtain a high single-mode yield, a $\lambda/4$ phase-shift structure is placed in the middle of the DFB section. The light emitted from the DFB section is reflected back by the DBR section, which helps increase the optical power. Moreover, the feedback from the DBR section can further increase the yield of single-mode emission. As shown in Fig. 2(a), the two sections of the device have the same InGaAlAs MQWs, which greatly simplifies device fabrication.

Results and Discussions The threshold current of the laser at 20 ℃ is 12 mA. The optical power is 18 mW at the injection current of 100 mA [Fig. 3(a)]. The emission wavelength of the laser is approximately 1320 nm. The side-mode suppression ratio of the optical spectra is larger than 50 dB when the DFB current increases from 30 mA to 90 mA [Fig. 3(b)]. At 20 ℃, the 3-dB small signal direct modulation bandwidth of the laser is 20 GHz at the injection current of 60 mA and increases to 29 GHz when the current increases to 90 mA [Fig. 4(a)]. By fitting the experimental modulation response curve, the intrinsic modulation bandwidth is found to be 35.4 GHz at the current of 94 mA, indicating that the modulation bandwidth of the laser can be further enhanced by optimizing the laser design and fabrication process. The frequency of the relaxation oscillations, which is also obtained by fitting the experimental modulation response data, increases with the injection current at the rate of 0.25 GHz/mA. 25-Gbit/s nonreturn to zero (NRZ) data transmissions using the laser are conducted. Data patterns having a $2^{15}-1$ length are generated by a commercial pulse pattern generator. Clear open eye views can be obtained after 10 km transmission (Fig. 5). The bit error rate (BER) performance of the transmission is also analyzed. The 10-km transmission power penalty of obtaining BER of 10^{-10} is less than 1 dB at both 20 ℃ and 80 ℃ (Fig. 6).

Conclusions A high-speed directly-modulated DFB laser integrated with a DBR section working at 1.3-μm wavelength is fabricated using InGaAlAs/InP multi-quantum wells as the active material. For the cavity length of 200 μm, the 3-dB small signal direct modulation bandwidth of the laser is larger than 29 GHz. Under 25-Gbit/s NRZ data direct modulation, the power penalty to obtain the BER of 10^{-10} after single-mode fiber transmission of 10 km is less than 1 dB at both 20 ℃ and 80 ℃. A longer active region length of the device is beneficial for improving the output slope efficiency and reducing the adverse effects of current heating. The fabricated device is a promising light source for short-reach, high-capacity optical communication systems.

Key words lasers; semiconductor lasers; high speed direct modulation; InGaAlAs/InP quantum wells; 1.3 μm band